JMEPEG (2006) 15:596-600
DOI: 10.1361/105994906X136133

1059-9495/$19.00

Preparation and Properties of Alloy 2618 Reinforced by Submicron AlN Particles

J.H. Wang and D.Q. Yi

(Submitted February 15, 2005; in revised form November 17, 2005)

An attempt was made to explore the possibility of fabricating AA2618 reinforced by submicron AlN particles. The results show that the addition of AlN particles decreases remarkably the grain size of the alloy. The 2618-AlN dispersion-strengthened alloy has the same strength as AA2618 at room temperature in the T6 state, but exhibits significantly higher strength after isothermal exposure at 200 °C for 100 h. The strength of the dispersion-strengthened alloy at elevated temperatures was greater than that of AA2618.

Keywords aluminum alloy, casting, mechanical properties, microstructures

1. Introduction

AA2618 is a heat-treatable Al-Cu-Mg-Fe-Ni forging alloy, which is widely used in the automobile industry and for aircraft engine components (Ref 1). It is a heat-resistant structural material fabricated by ingot metallurgy (I/M). The addition of small amounts of Fe and Ni can improve the microstructural stability during thermal exposure (Ref 2). The main precipitates in this alloy are coherent Guinier-Preston-Bagaryatskii (GPB) zones, which form rapidly during aging at temperatures higher than 200 °C, and the semicoherent S′(Al_2CuMg) phase, which apparently strengthens the alloy. Stable intermetallic particles, such as the Al_9FeNi particles, are useful in controlling grain size and for impeding dislocation motion. It should be stressed here that the amount of Fe and Ni in the alloy should be balanced; otherwise, these elements may combine with Cu to form stable compounds that reduce the response of the alloy to age hardening (Ref 3). To improve the mechanical properties of AA2618 at high temperatures, much research has been done over the years (Refs 4-11). The addition of Sc and Zr to AA2618 results in the precipitation of primary $Al_3(Sc,Zr)$ particles, and thus, increases both the ambient- and elevated-temperature strength (Refs 4, 5). Increasing the amount of Fe and Ni in the alloy enhances the tensile strength (Refs 6, 7). The experimental results indicate that AA2618, reinforced with 5 to 20 wt.% SiC or Al_3O_2 particles in the size range of 2 to 20 μm, showed higher elevated-temperature tensile strength (Refs 8, 9). However, the SiC and Al_3O_2 particles do not bond well with the matrix due to the poor wetting ability between particles and matrix. Additionally, stress concentrations near the coarse particles are high, resulting in the tendency for premature rupture along the interface. The particles are also prone to fracture when the composite is subjected to deformation. The fracture tendency of the coarse particles depends on their aspect ratio (Ref 12). Conversely, there is no problem with wetting in AA2618 reinforced with in-situ synthetic TiC particles (Ref 13), but the processing is so complicated it results in high manufacturing costs. The purpose of the present study is to explore the possibility of fabricating AA2618 reinforced with submicron AlN particles using stir casting as the processing method, and to investigate the effect of the AlN particles on microstructure and mechanical properties of the alloy, especially the elevated-temperature mechanical properties.

J.H. Wang, Institute of Materials Research, School of Mechanical Engineering, Xiangtan University, Xiangtan 411105, People's Republic of China; and **D.Q. Yi,** Institute of Material Science and Engineering, Central South University, Changsha 410083, People's Republic of China. Contact e-mail: super_wang111@hotmail.com.

Table 1 Compositions of the alloys used in this study (wt.%)

Alloy	Cu	Mg	Fe	Ni	Ti	AlN	Al
AA2618	2.26	1.53	1.1	1.15	0.02	0	bal
2618-AlN	2.26	1.53	1.1	1.15	0.02	1.0	bal

Note: The volume fraction of AlN is 0.83%.

2. Experimental Procedures

The nominal compositions of the studied materials are listed in Table 1. The reinforced AA 2618 is referred to 2618-AlN in the following discussions. Pure Al and Mg, and master alloys of Al-Cu, Al-Fe, and Al-Ni, were used as starting materials. One piece of AA2618 was used as the reference material. The fabricating method for 2618-AlN consists of melting a multiplex-salt (30%NaCl + 47%KCl + 23%Na_3AlF_6) in a resistance crucible while the submicron (0.1-0.7 μm, mean size 0.4 μm) AlN particles were preheated at 250 °C to remove residual moisture. A mixture of 50 wt.% multiplex-salt and 50 wt.% submicron AlN particles was ball milled for 2 h. The AA2618 was then melted at 750 °C and kept molten for 20 min in a resistance crucible furnace at which point 2 wt.% of the salt-AlN mixture was added to the alloy and stirred for a sufficient time to ensure complete mixing. After refining and inoculation, the molten alloy was poured at 730 °C into a preheated steel mold (200 °C). The cast ingots were homogenized at 480 °C for 16 h. The ingots were sectioned into 16 mm thick

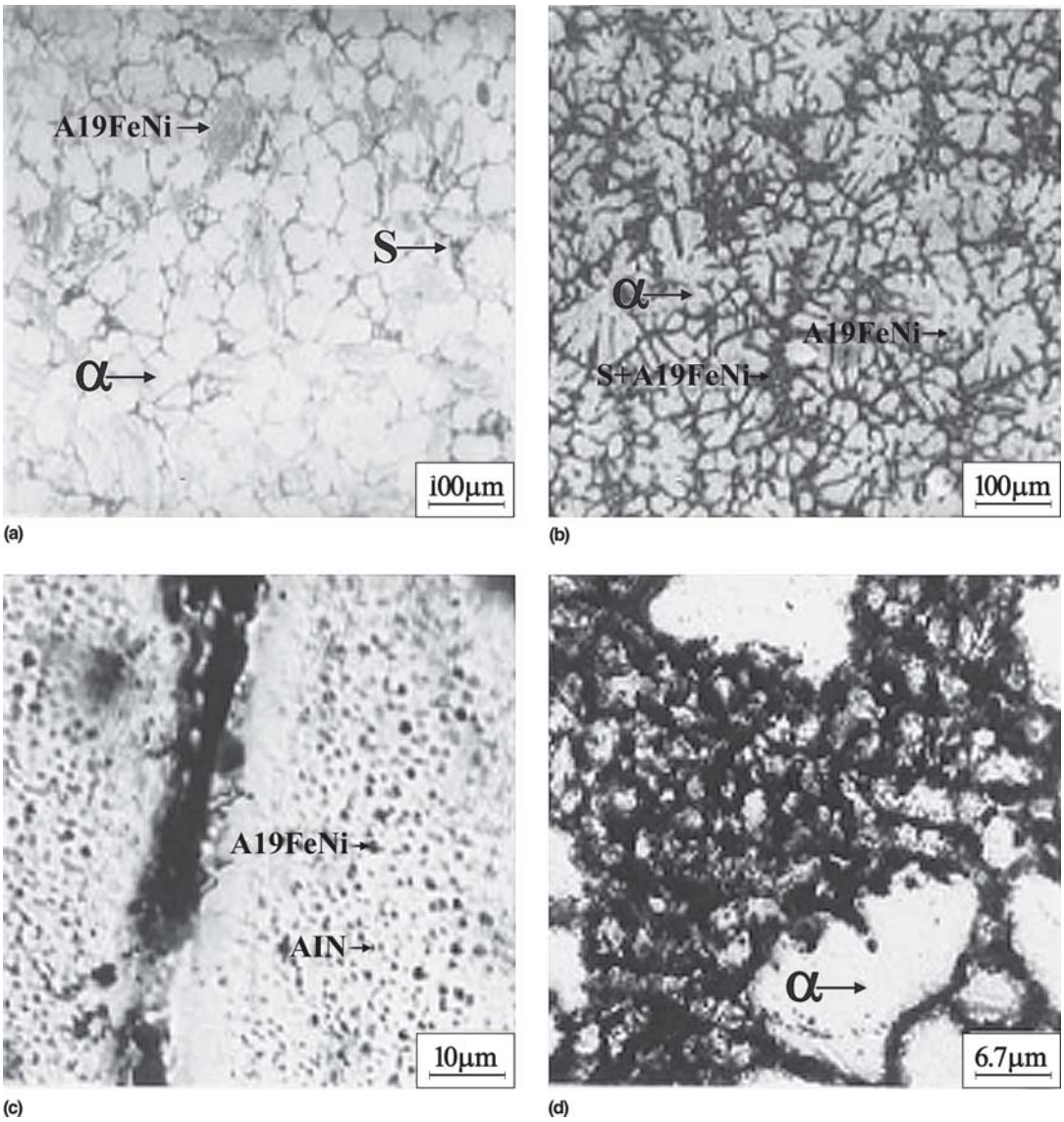

Fig. 1 Microstructures of the as-cast alloys: (a) AA2618; (b-d) 2618-AlN

plates and rolled to 7 mm in three passes using a reheat temperature of 480 °C. The plates were subsequently rolled to a thickness of 2 mm in three passes at room temperature with the plates annealed at 450 °C between passes. The rolled plates were then solutionized in salt at 535 °C and quenched into water at room temperature. The plates were then aged at 200 °C for 20 h (T6 state). After aging, some of the material was isothermally aged at 200 °C for 100 h in a resistance furnace to examine the effects of long-term high temperature exposure on the room- and elevated-temperature mechanical properties of the alloys. The gauge section of the tensile specimens measured 30 × 6 × 2 mm.

The microstructures of the alloys were observed using optical microscopy (OM) and transmission electron microscopy (TEM). X-ray diffraction (XRD) was carried out to check the phase constitution of 2618-AlN. The samples for TEM observation were prepared by double-jet electro-chemical polishing in a solution of 25% nitric acid and 75% methyl alcohol at −15 to −25 °C. The room- and elevated-temperature tensile tests were carried out on an Instron (Instron Company, UK) 8032 servo-hydraulic testing system attached to a computerized data acquisition system. The tensile specimens were heated to the test temperature and kept there for 12 min prior to tensile testing. The displacement rate was 2 mm/min, yielding a strain rate 0.067/min.

3. Results and Discussion

3.1 Microstructures of the Alloys

Figure 1(a) and (b) show the microstructures of as-cast AA2618 and 2618-AlN. Three phases, α(Al) and S (Al_2CuMg), as well as Al_9FeNi, were identified in the alloys. Besides these phases, the AlN particles (gray) can be seen in 2618-AlN, as shown in Fig. 1(c). Figure 1(d) shows the morphology of the boundary in 2618-AlN. Due to the limited fraction of AlN particles, they cannot be identified from the XRD pattern, as shown in Fig. 2. In AA2618, the Al_9FeNi phase is distributed inside the grains or at the grain-boundaries in needle-like form, but the S (Al_2CuMg) phase is found only at the grain boundaries. In 2618-AlN, most of the coarse Al_9FeNi and S (Al_2CuMg) phases are observed at the grain boundaries,

and the morphology of the Al_9FeNi phase is "block-like". The morphologies of the grains of 2618-AlN is petaline in nature, and the subgrain size is slightly smaller than that of AA2618 (Fig. 1b).

The wetting ability of the submicron AlN particles with liquid Al was improved due to the use of the multiplex-salt (NaCl + KCl + Na3AlF6), and the high-energy ball milling salt-particle mixture. During the melting of 2618-AlN, the mixture dispersed rapidly on the surface of the liquid aluminum alloy due to the multiplex-salt. Stirring continuously, the AlN particles were evenly distributed in the liquid alloy. After solidification, the AlN particles were uniformly dispersed in 2618-AlN. A TEM micrograph of 2618-AlN after quenching is shown in Fig. 3. It is clear that many AlN particles are dispersed in the α (Al) matrix of 2618-AlN.

The S (Al_2CuMg) phase that existed at the grain boundaries of AA2618 and 2618-AlN dissolved after homogenization at 480 °C, and precipitated in the alloys after cooling. The morphology of Al_9FeNi phase was that of small particles after hot-rolling and this did not change during subsequent annealing treatments. The microstructures of hot-rolled AA2618 and 2618-AlN are shown in Fig. 4. It can be seen that dynamic recrystallization has occurred in both alloys during hot rolling. The grain size of 2618-AlN is smaller than that of AA2618 after dynamic recrystallization owing to the existence of the large fraction of dispersed submicron AlN particles, which suppressed dynamic recrystallization as well as coarsening of the grain of 2618-AlN.

The force exerted by the AlN particles in retarding recrystallization can be expressed as (Ref 14):

$$\mathbf{Pz} = 3\mathbf{f}\boldsymbol{\gamma}/2\mathbf{r} \quad \text{(Eq 1)}$$

where $\boldsymbol{\gamma}$ is the boundary energy (given a value of 0.5 J/m^2), **f** is the volume fraction (0.83%), and **r** is the average size of the AlN particles (4×10^{-7} m). According to the calculation, the force **Pz** exerted by the AlN particles is equal to 15.6 MPa. The force resisting recrystallization in 2618-AlN is larger than that of AA2618 due to the fraction of AlN particles. Likewise, the velocity of the grain boundaries in 2618-AlN is smaller than that of AA2618 for the same reason.

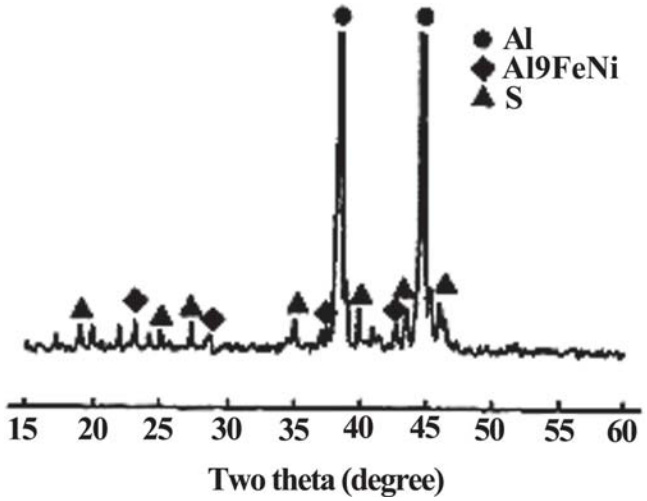

Fig. 2 XRD pattern of 2618-AlN

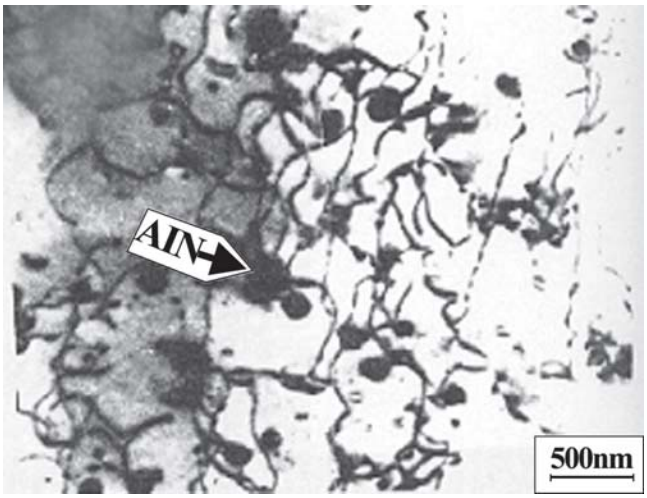

Fig. 3 TEM observation of alloy 2618-AlN after quenching

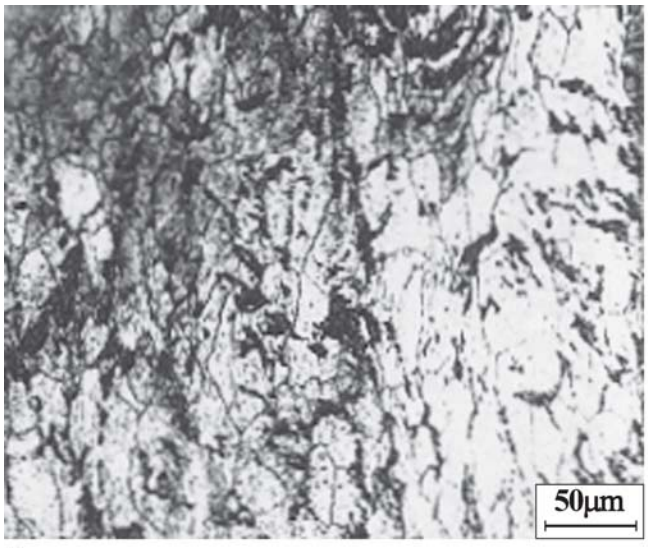

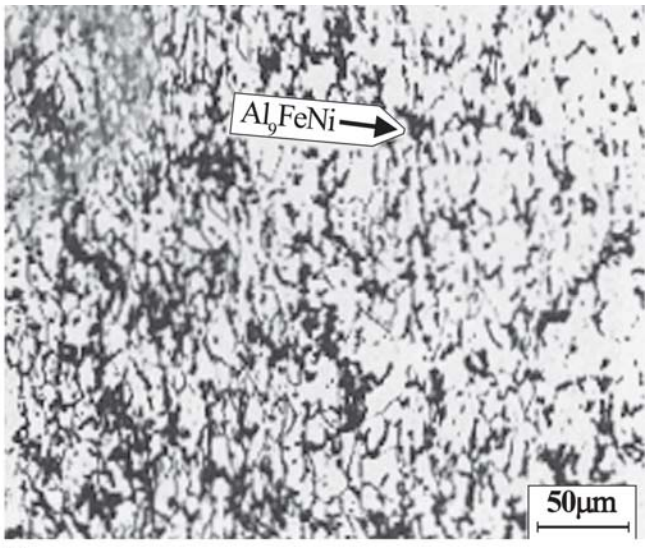

Fig. 4 Microstructures of hot-rolled (a) AA2618 and (b) 2618-AlN

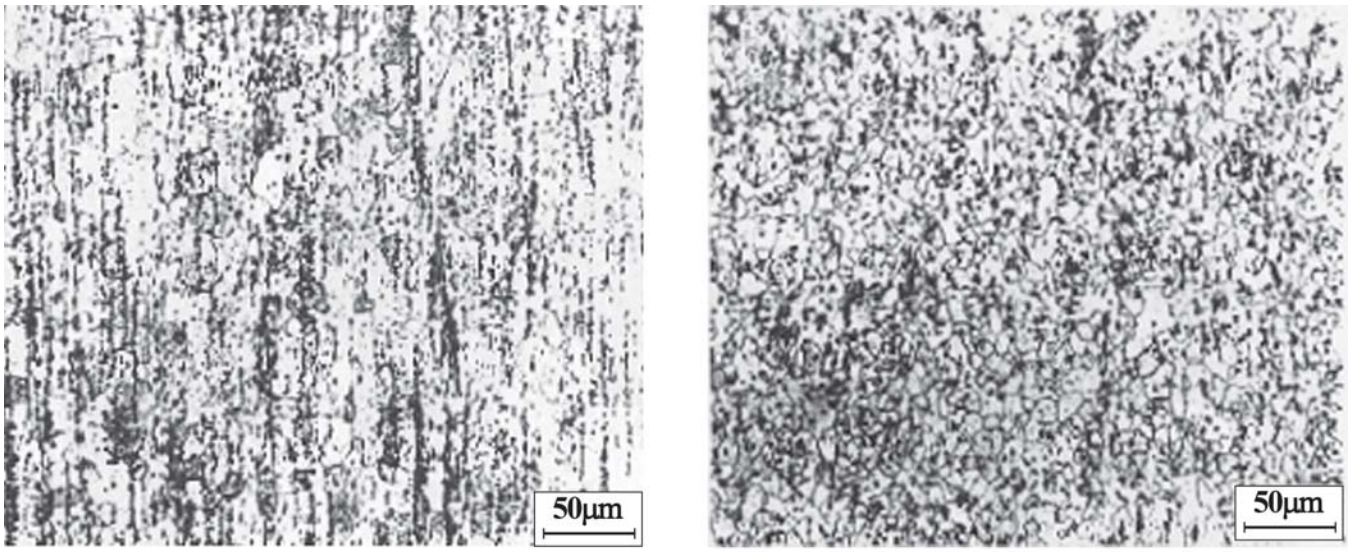

(a) (b)

Fig. 5 Microstructures of the quench-aged alloys (a) AA2618 and (b) 2618-AlN

The microstructures of AA2618 and 2618-AlN in the T6 state are shown in Fig. 5. This figure shows that recrystallization occurred in both alloys with the grain size of both alloys becoming larger during solid-solution heat treatment (at 535 °C) and long-term aging. The measured results of the alloys show that the mean grain size of AA2618 is about 25 μm and that of 2618-AlN 12 μm. It can be seen from Fig. 5 that the grain size of 2618-AlN is much smaller than that of AA2618. The reason is the same as that explained previously in this article.

3.2 Properties of AA2618 and 2618-AlN

The room-temperature mechanical properties of AA2618 and 2618-AlN after quench-aging (T6 state) and isothermal exposure at 200 °C for 100 h are shown in Table 2. Clearly, the tensile strength of 2618-AlN is almost equal to that of AA2618 in the T6 state. It can be inferred from the experimental results that the existence of the semicoherent S′ (Al_2CuMg) phase is the main reason for the strengthening of the alloys (T6 state) at room temperature. There is little strengthening from the submicron AlN particles or the smaller grain size of the matrix for 2618-AlN in the T6 state. However, after exposed at 200 °C for 100 h, the room-temperature tensile strength of 2618-AlN became larger than that of AA2618. The reasons for this are that S′ (Al_2CuMg) coarsened and gradually transformed to the equilibrium S (Al_2CuMg) phase, which is no longer coherent with the α (Al). So strengthening from the semicoherent S′ phase was almost completely lost after isothermal exposure. Due to the existence of the fraction of submicron AlN particles and their strengthening of 2618-AlN, the room-temperature tensile strength of 2618-AlN was larger than that of AA2618.

The elevated temperature tensile properties of the alloys are shown in Table 3. With the addition of submicron AlN particles, the elevated temperature tensile strength of 2618-AlN increased markedly regardless of whether it was subjected to isothermal exposure at 200 °C or not. The results show that the elevated temperature tensile strength of 2618-AlN was 19% higher than that of AA2618 before isothermal exposure. After isothermal exposure at 200 °C for 100 h, the strength increased by 30% relative to AA2618. The results indicate that strengthening from S′ decreased significantly at elevated temperatures for AA2618, while the AlN particles helped keep the strength of 2618-AlN high relative to AA2618. After isothermal exposure, the tensile strength of AA2618 and 2618-AlN decreased to a greater degree during elevated temperature testing for the reasons expressed previously in this article. However, the submicron AlN particles, which are stable at high temperatures, are still effective, retarding dislocation movement and providing higher strength than AA2618. The mechanism is Orowan strengthening whereby a moving dislocation encounters a hard particle, for example, AlN particles, and must bypass it by some mechanism (i.e., particle looping or climb). The stress required to move a dislocation around a particle is given by the expression (Ref 15):

$$\tau = 2Gb/\lambda \quad \text{(Eq 2)}$$

Table 2 Room temperature mechanical properties of the alloys

	RT T6 Condition			Exposure at 200 °C for 100 h		
Alloy	σ_b/MPa	σ_S/MPa	δ/%	σ_b/MPa	σ_S/MPa	δ/%
AA2618	409	369	15.4	316	311	18.8
2618-AlN	411	371	14.5	348	332	16.7

Table 3 Elevated temperature mechanical properties of the alloys

	200 °C			200 °C (after isothermal exposure)		
Alloy	σ_b/MPa	σ_S/MPa	δ/%	σ_b/MPa	σ_S/MPa	δ/%
AA2618	230	203	22.4	183	158	24.4
2618-AlN	274	241	19.5	238	205	21.1

where **G** (given a value of 6×10^4 MPa) is the shear modulus and **b** (2.8683×10^{-10}m) is the Burger's vector. λ is the interparticle spacing (2.674×10^{-7} m), which decreases due to the existence of a high fraction of submicron AlN particles in 2618-AlN. According to Eq 2, the calculated τ exerted by AlN particles is 12.9 MPa. Due to the effect of AlN particles, the elevated temperature strength of 2618-AlN would be higher than that of AA2618.

4. Conclusions

The following conclusions can be drawn from the current study:

- The AlN particles can be uniformly distributed in 2618-AlN by using a mixture of multiplex-salt (NaCl + KCl + Na_3AlF_6) and submicron AlN particles through stir casting.
- The addition of 1.0 wt.% submicron AlN particles to AA2618 can remarkably decrease the grain size of the alloy by pinning grain boundaries during recrystallizations and grain growth.
- The room temperature tensile strength of 2618-AlN is almost equal to that of AA2618 in the T6 condition, and before exposure at 200 °C for 100 h, 2618-AlN is mainly dependent on the strengthening imparted by S′ (Al_2CuMg).
- A large fraction of dispersed submicron AlN particles, which are stable at high temperature, increase the elevated temperature tensile strength of 2618-AlN at 200 °C, after exposure at 200 °C for 100 h, relative to AA2618.

Acknowledgments

The authors gratefully acknowledge the financial support of the National Key Basic Research and Development Program of China (G1999064909) and wish to give thanks to Editor Jeff Hawk, Dr. X.G. Lu, and Dr. Z.C Li for their contributions to this article.

References

1. W. Zhutang and T. Rongzhang, *Handbook of Aluminum Alloys and Processing,* Changsha, Central South University of Technology Press, 1989
2. I. Oguocha and S. Yannacopolos, The Structure of Al_xFeNi Phase in Al-Cu- Mg-Fe-Ni Alloy (AA2618), *J. Mater. Sci.,* 1996, **31**(9), p 5615-5618
3. I. Oguocha and S. Yannacopoulos, Precipitation and Dissolution Kinetics in Al-Cu-Mg-Fe-Ni alloy 2618 and Al-Alumina Particle Metal Matrix Composite, *Mater. Sci. Eng. A,* 1997, **231,** p 25-33
4. Y. Kun, L. Songrui, and L. Wenxian, Recrystallization Behavior in an Al-Cu-Mg-Fe-Ni Alloy with Trace Scandium and Zirconium, *Mater. Trans. JIM,* 2000, **41**(2), p 358-364
5. Y. Kun, L. Wenxian, L. Songrui, and Z. Jun, Mechanical Properties and Microstructure of Aluminum Alloy 2618 with Al_3(Sc,Zr) Phases, *Mater. Sci. Eng. A,* 2004, **36,** p 88-93
6. J. Wang and D. Yi, Effect of Melt Over-Heating and Zirconium Alloying on the Morphology of Al_9FeNi Phase and Mechanical Properties of 2618 Alloy, *Acta Metall. Sinica (English Letters),* 2002, **125**(6), p 525-529
7. J. Wang, D. Yi, and B. Wang, Microstructure and Properties of Alloy 2618-Ti Heat Resistant Aluminum Alloy, *Trans. Nonferrous Met. Soc. China,* 2003, **13**(3), p 590-595
8. B.Y. Zong and B. Derby, Creep Behaviour of a SiC Particulate Reinforced Al-2618 Metal Matrix Composite, *Acta Mater.,* 1997, **45**(1), p 41-49
9. P. Cavaliere, E. Cerri, and P. Leo, Hot Deformation and Processing Maps of a Particulate Reinforced 2618/$Al_2O_3/20_p$ Metal Matrix Composite, *Composites Sci. Technol.,* 2004, **64**(9), p 1287-1291
10. R.P. Underhill, P.S. Grant, and B. Cantor, Microstructure of Spray-Formed Al Alloy 2618, *Mater. Des.,* 1993, **14,** p 45-47
11. F. Bardi, M. Cabibbo, and S. Spigarelli, An Analysis of Thermo-Mechanical Treatments of a 2618 Aluminum Alloy: Study of Optimum Conditions for Warm Forging, *Mater. Sci. Eng. A,* 2002, **334,** p 87-95
12. P. Poza and J. Llorca, A study of the failure mechanisms in Al/Al_2O_3 and Al/SiC composites through quantitative microscopy, *J. Mater. Sci.,* 1995, **30,** p 6075-6080
13. L. Chunguang, Z. Houan, and P. Xiuxia, Aging Characteristic and Mechanical Properties of TiC/2618 Composite, *Trans. Nonferrous Met. Soc. China,* 2001, **11**(6), p 920-924
14. W. Mao and X. Zhang, *Recrystallization and Growth of Metals,* Beijing, Metallurgy Industry Publishers, 1994, p 77-102, in Chinese
15. S. Singh and D.B. Goel, Influence of Thermomechanical Ageing on Tensile Properties of 2014 Aluminium Alloy, *J. Mater. Sci.,* 1990, **25**(9), p 3894-3900